THE JOURNAL OF BIOLOGICAL CHEMISTRY
Vol. 275, No. 22, Issue of June 2, pp. 16871–16878, 2000

Printed in U.S.A.

Folding Pathway Mediated by an Intramolecular Chaperone

THE INHIBITORY AND CHAPERONE FUNCTIONS OF THE SUBTILISIN PROPEPTIDE ARE NOT OBLIGATORILY LINKED*

Received for publication, December 6, 1999, and in revised form, February 15, 2000

Xuan Fu, Masayori Inouye, and Ujwal Shinde‡

From the Department of Biochemistry, Robert Wood Johnson Medical School-University of Medicine and Dentistry of New Jersey, Piscataway, New Jersey 08854

The subtilisin propeptide functions as an intramolecular chaperone (IMC) that facilitates correct folding of the catalytic domain while acting like a competitive inhibitor of proteolytic activity. Upon completion of folding, subtilisin initiates IMC degradation to complete precursor maturation. Existing data suggest that the chaperone and inhibitory functions of the subtilisin IMC domain are interdependent during folding. Based on x-ray structure of the IMC-subtilisin complex, we introduce a point mutation (E112A) to disrupt three hydrogen bonds that stabilize the interface between the protease and its IMC domain. This mutation within subtilisin does not alter the folding kinetics but dramatically slows down autoprocessing of the IMC domain. Inhibition of E112A-subtilisin activity by the IMC added *in trans* is 35-fold weaker than wild-type subtilisin. Although the IMC domain displays substantial loss of inhibitory function, its ability to chaperone E112A-subtilisin folding remains intact. Our results show that (i) the chaperone activity of the IMC domain is not obligatorily linked with its ability to bind with and inhibit active subtilisin; (ii) degradation and not autoprocessing of the IMC domain is the rate-limiting step in precursor maturation; and (iii) the Glu^{112} residue within the IMC-subtilisin interface is not crucial for initiating folding but is important in maintaining the IMC structure capable of binding subtilisin.

Subtilisin E is an alkaline serine protease found in *Bacillus subtilis* (1). *In vivo* this protein exists as a precursor, namely pre-pro-subtilisin (1). The presequence acts as a signal peptide and facilitates the secretion of pro-subtilisin across the cytoplasmic membrane, whereas the pro-region or propeptide functions as an intramolecular chaperone (IMC)[1] that guides correct folding of the subtilisin domain (2–4). Upon completion of folding the precursor removes the IMC domain through autoproteolysis to give active subtilisin (5).

Similar folding mechanisms exist in numerous prokaryotic and eukaryotic proteases (6) that include subtilisin (2–4), α-lytic protease (7, 8), aqualysin (9, 10), carboxypeptidase Y (11, 12), cathepsin L (13), and thermolysin (14). In addition to proteases, a variety of other proteins such as nerve growth factor (15), amphiregulin (16), and activin A (17) mature from higher molecular weight precursor proteins. Although propeptides of several proteins can function as IMCs, not all propeptides can directly catalyze folding reactions (18, 19). Such propeptides can exert their biological functions using a myriad of mechanisms (19). Close scrutiny of such propeptides suggests that they may actually be post-translational "modulators" of protein function because they are directly or indirectly involved in the structural organization (20). The conservation of propeptide function across unrelated protease families suggests that, similar to proteases, propeptides may have evolved in multiple parallel pathways and may share a similar mechanism of action (18). It is also possible that propeptides have evolutionarily preceded the formation of the protease families (21).

IMC-mediated protein folding is best understood in subtilisin and α-lytic protease (20). The *in vitro* folding pathway of prosubtilisin involves precursor folding (22, 23), followed by autoprocessing (24) that coincides with structural changes that lead to degradation of the IMC domain (23). Folding of denatured subtilisin in the absence of its IMC domain traps the protease into an inactive molten-globule like intermediate state (8, 23, 25, 26). Addition of the IMC domain *in trans* helps this intermediate adopt an active conformation (8, 25). Recent data show that the IMC domain can impart structural information onto its protease (27) and that this imprinting occurs after autoprocessing but before degradation of the IMC from the precursor (28). Such results suggest that IMCs promote protein folding by direct stabilization of the rate-limiting folding transition state and support the notion that the IMC is essential only during late stages of the folding process (29, 30).

Amino acid residues Asp^{32}, His^{64}, and Ser^{221} constitute the catalytic triad of subtilisin and mediate both autoprocessing and degradation of the IMC domain (3–5, 31). However, these two activities are distinctly different from one another. As a result the IMC-S221C-subtilisin can autoprocess its IMC domain but is unable to degrade it, resulting in the formation of a stable IMC-subtilisin complex (31). The 2 Å resolution x-ray structure of such a complex was recently solved (32, 33). It is evident from this structure that degradation of the IMC domain subsequent to autoproteolysis is essential because the C-terminal end of the IMC domain interacts with the substrate-binding loop of the protease through numerous hydrogen bonds. The C-terminal end therefore inhibits the enzymatic activity of the protease by steric occlusion of its active site (32, 33). However, the proteolysis of even a single peptide bond within the IMC can dramatically decrease its affinity for the protease domain resulting in protease activation (34). It is important to note that the IMC domain and its fragments are devoid of secondary and tertiary structures when isolated from

* This work was supported by National Institutes of Health Grant GM-56419-03 (to M. I.). The costs of publication of this article were defrayed in part by the payment of page charges. This article must therefore be hereby marked "*advertisement*" in accordance with 18 U.S.C. Section 1734 solely to indicate this fact.

‡ To whom correspondence should be addressed: Dept. of Biochemistry, Robert Wood Johnson Medical School-UMDNJ, 675 Hoes Ln., Piscataway, NJ 08854. Tel.: 732-235-3342; Fax: 732-235-4783; E-mail: shinde@rwja.umdnj.edu.

[1] The abbreviations used are: IMC, intramolecular chaperone; ANS, anilino-8-napthalene sulfonic acid; PMSF, phenylmethylsulfonyl fluoride; DTT, dithiothreitol.

subtilisin (22, 25, 35). Hence, specific interactions between IMC-subtilisin appear to be important to stabilize the complex.

Results obtained through mutational studies within the IMC domain suggest the existence of a direct correlation between the chaperone function and the inhibition of proteolytic activity (34, 35). In the present manuscript we maintain the IMC domain intact but destroy three specific hydrogen bonds that exist between the Glu^{112} and the backbone of the IMC domain. These H bonds, along with hydrophobic interactions, appear to dominate the forces that stabilize the IMC-subtilisin complex. Our results indicate that the E112A substitution does not affect the folding of IMC-E112A-subtilisin. This mutant precursor undergoes efficient processing into an active protease, and the substitution does not significantly affect maturation. However, the autoprocessing and degradation of the IMC domain are dramatically altered. This result is attributed to the inability of the precursor to form a stable IMC-subtilisin complex because of E112A mutation. Hence, the IMC becomes a poor competitive inhibitor of the mutant subtilisin as the K_i value is increased approximately 35-fold, and these results show that the chaperone and inhibitory functions of the IMC domain are not obligatorily related.

EXPERIMENTAL PROCEDURES

Materials

The site-directed mutagenesis kit was purchased from Strategene Inc. The hydrophobic dye, 1-anilino-8-napthalene sulfonic acid (ANS), phenylmethylsulphonyl fluoride (PMSF), and the synthetic substrate for subtilisin, succincyl-Ala-L-Ala-L-Pro-Phe-*p*-nitroanilide, were purchased from Sigma.

Methods

Site-directed Mutagenesis—The oligonucleotide primers were synthesized at 0.2 μM scale on an Applied Biosystems (Foster City, CA) 380B synthesizer using reagents obtained from Applied Biosystems Inc. Purification of these oligonucleotides was done using oligo-purification cartridges supplied by Applied Biosystems Inc. The concentrations of the oligonucleotides were estimated spectrophotometrically by recording the absorbance at 260 nm. These oligonucleotides were used to introduce the desired mutations into plasmids pET11a-pro-sub (27) and pET11a-proS221C-sub (31, 34) using the QuikChange site-directed mutagenesis kit purchased from Strategene Cloning Systems. The mutations were subsequently confirmed through DNA sequencing performed on an Applied Biosystems Inc.-310 Genetic Analyzer purchased from Applied Biosystems Inc.

Expression of Wild-type and the Active Site Mutant of Pro-subtilisin—Plasmids pET11a-pro-sub and pET11a-proS221C-sub were transformed into *Escherichia coli* strain BL21(DE3) and grown in M9 medium supplemented with 50 μg/ml ampicillin (27). At an absorbance of 0.8 $A_{600\ nm}$, the proteins were induced by adding isopropyl-1-thio-β-D-galactopyranoside (final concentration, 1 mM). After 4 h at 37 °C, the cells were harvested by centrifugation and washed twice with a wash buffer containing 20 mM Tris-HCl, pH 7.0, and 150 mM NaCl. The cells were resuspended in 30 ml of wash buffer supplemented with 20 μl of a mixture of protease inhibitors (1 mg/ml each) and DNase I. The suspension were lysed at 4 °C using a French press cell (10,000 p.s.i.). The lysate was centrifuged at 20,000 $\times$ *g* for 20 min, and the supernatant and pellet were separated. Because the constructs are under the control of the T7 promoter, the levels of expression are very high (~50 mg/liter of culture). As a result, the induced protein was localized in inclusion bodies (27, 28, 31). After confirming that the protein of interest was located inside the inclusion bodies, the pellets were rinsed twice with wash buffer to carefully remove traces of cell lysate. The pellet was solubilized in 30 ml of 6 M guanidine hydrochloride, pH 4.8, by sonication. The solution was incubated overnight (with constant shaking) at 4 °C. Insoluble debris was removed by centrifugation (100,000 $\times$ *g* for 2 h), and the supernatant was used to purify the proteins.

Purification of the Precursors—The supernatant was dialyzed overnight at 4 °C against 100 volumes of Buffer A (50 mM sodium phosphate buffer, pH 5.0, containing 5 M urea) with one buffer change. The dialyzed protein was centrifuged (100,000 $\times$ *g* for 2 h) to remove precipitated proteins. Soluble protein was applied to a CM-Sephadex C-50 column (3 $\times$ 30 cm) that was equilibrated with Buffer A. The column was washed with Buffer A until proteins were no longer detected in the flow-through, and the protein was eluted using a NaCl gradient in Buffer A. Wild-type pro-subtilisin eluted between 0.15 and 0.2 M NaCl, and fractions containing the precursors were pooled and concentrated to approximately 2.0 ml by an Amicon ultrafiltration system using a YM10 membrane. The proteins were dialyzed as described earlier, but this time using Buffer B (50 mM Tris-HCl, pH 8.0, containing 5 M urea). The protein were again centrifuged (100,000 $\times$ *g* for 2 h), and the supernatant was applied to a QAE-Sephadex Q-50 column (1.5 $\times$ 15 cm) that was pre-equilibrated with Buffer B. After thoroughly washing the column with Buffer B, proteins were eluted using a gradient of 0–0.4 M NaCl in Buffer B. Fractions containing the precursor were pooled and concentrated as described earlier. Protein samples were finally dialyzed against 50 mM sodium phosphate buffer, pH 7.0, containing 5 M urea and stored at −20 °C until use.

Folding through Rapid Dilution—The precursor proteins (1.25 mg/ml) were denatured in 6 M guanidine hydrochloride, pH 4.8. The temperature for renaturation was maintained at 4 °C, and folding was initiated through rapid dilution of 200 μl of the protein into 2800 μl of 50 mM Tris-HCl, pH 7.0, containing 0.5 M $(NH_4)_2SO_4$, 1 mM $CaCl_2$, 5 mM DTT. The kinetics of folding were monitored by rapidly diluting the denatured precursors (15-fold dilution) into a quartz cuvette (1-cm path length) and simultaneously recording the changes in CD spectra at 222 nm. Data were collected at 1-s time intervals with a bandwidth of 3 nm. Each kinetic trace was recorded for 3000 s and represents the average of three independent experiments. By using nonlinear regression the traces were found to fit a single exponential rate constant. The Prism Graph-Pad software, version 2.01, was used for the data fitting analysis and graph plotting.

Folding through a Stepwise Dialysis—Denatured proteins (100 μg/ml) are loaded into a dialysis tubing (12.0-kDa cut-off) and dialyzed against 100 volumes of 50 mM Tris-HCl, pH 7.0, containing 0.5 M $(NH_4)_2SO_4$, 1 mM $CaCl_2$, 5 mM DTT that contains 4 M urea. After 4 h, the buffer was replaced with one containing 3 M urea. This procedure is repeated in a stepwise manner until complete removal of urea is achieved (23, 27, 28, 31). The proteins were allowed to incubate in the final buffer for up to 1 week (31) and then concentrated using an ultrafiltration unit with a YM10 membrane.

Enzymatic Activity of the Protease Domain—An aliquot of the sample is incubated at 37 °C in 200 μl of 50 mM Tris-HCl, pH 8.5, containing 1 mM $CaCl_2$. For measuring the K_m the substrate concentrations were varied between 0.05 and 2.5 mM succinyl-Ala-Ala-Pro-Phe-*p*-nitroanilide. Enzymatic activity of subtilisin is estimated by monitoring the release of *p*-nitroaniline through changes in absorbance at 405 nm (34). Readings are collected at 12-s time intervals using a Bio-Rad UV microplate reader to estimate the reaction velocity. One unit is defined as the activity releasing 1 μM of *p*-nitroaniline/min. An A_{405} of 8.5 corresponds to 1 mM of *p*-nitroaniline.

Circular Dichroism Studies—CD measurements were performed on an automated AVIV 60DS spectrophotometer maintained at 4 °C. The spectra were taken from 260 to 190 nm. The protein concentration was 0.3 mg/ml, and a path length of 0.1 cm was used. In thermal denaturing measurements, temperatures were increased from 10 to 90 °C at 0.5 °C intervals, equilibrated for 6 s at each temperature. Data were collected at each temperature for 5 s. Folding kinetics were monitored by rapidly diluting 200 μl of precursor proteins (1.25 mg/ml) into 2800 μl of buffer and simultaneously monitoring changes in the CD absorbance at 222 nm.

Fluorescence Measurements—Fluorescence studies were carried out on an SLM Aminco Bowman Series 2 luminiscence spectrometer at 4 °C. Protein concentration was 100 nM and ANS concentration was 100 μM (27). The proteins were excited at 395 nm, and the emission scan was recorded from 410 to 600 nm. The excitation and emission bandwidths were maintained at 4 nm throughout the experiments. For the intrinsic fluorescence experiments, the proteins were excited at 295 nm, and the emission scans were recorded from 310 to 410 nm.

RESULTS AND DISCUSSION

The maturation pathway of subtilisin involves at least four distinct stages (28): (i) folding of the protease domain that is mediated by its IMC domain; (ii) autoprocessing of the peptide bond between the C terminus of the IMC domain and the N terminus of subtilisin; (iii) structural changes within the autoprocessed complex during which IMC continues to facilitate folding; and (iv) degradation of the IMC domain that renders maturation irreversible. Specific mutations within the catalytic

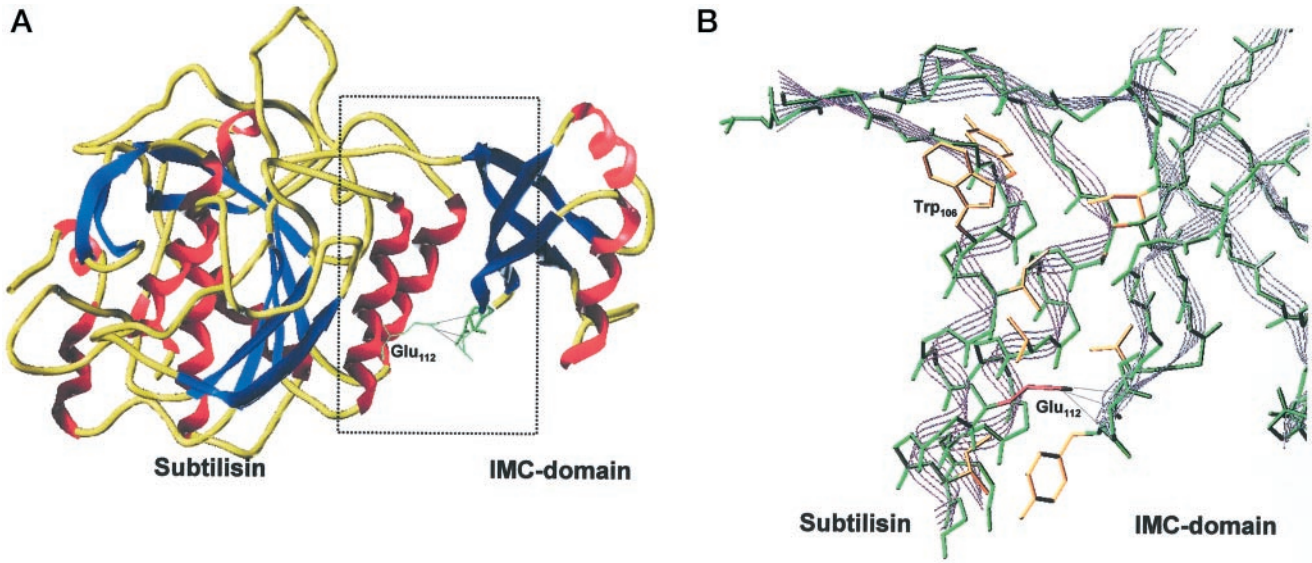

FIG. 1. **The x-ray structure of the autoprocessed IMC-S221C-subtilisin complex.** *A*, the ribbon and tube structure of the complex wherein the α-helices are displayed in *red*, β-sheets are in *blue*, and loop regions are in *yellow*. Residues involved in the H bonding that stabilize the side-on interaction of the IMC domain are depicted in *green*. *B*, the interface between the two parallel surfaces of the α-helices contributed by subtilisin and four anti-parallel β-sheets from the IMC domain. Hydrophobic residues that may stabilize the interface are shown in *yellow*, and the three hydrogen bonds are depicted by *dotted lines*.

triad of subtilisin facilitate the analysis of individual steps on this pathway. For example, when the catalytic residue Ser^{221} is substituted with Cys, the precursor undergoes folding, autoprocessing, and structural changes subsequent to its autocleavage to give a complex in which the IMC domain remains associated with subtilisin through noncovalent interactions (31).

Interactions That Stabilize the IMC-Subtilisin Complex—Fig. 1*A* depicts the x-ray structure of such an autoprocessed IMC-S221C-subtilisin complex (33), which is similar to the complex obtained by adding the IMC domain to folded subtilisin (32). The β-sheet of the IMC domain packs tightly against the two surface parallel α-helices of the mature domain. There are 26 hydrogen bonds that connect the IMC with mature subtilisin. These include the region of the IMC domain that interacts with the active site of subtilisin. The folded IMC domain has a compact structure with shape complementarity and high affinity to the protease domain (32, 33). Residue Glu^{112} forms three hydrogen bonds with the backbone of residues 42, 43, and 44 within the IMC domain and appears to play a major role in maintaining the IMC domain interactions with subtilisin in a "side-on" fashion (Fig. 1*B*). The interface is also stabilized by hydrophobic side chains between the interface of the β-sheets of the IMC domain and the two α-helices in subtilisin (Fig. 1*B*). On the basis of the structure of the complex, it has been proposed that the central αβα substructures within subtilisin were stabilized by the IMC domain (36). Hence, to understand the role of Glu^{112} in stabilizing interactions of the two parallel α-helices with the β-sheets in the IMC domain in an autoprocessed complex and to investigate its importance in the overall maturation process, this residue was substituted with an Ala using site-directed mutagenesis (see "Experimental Procedures"). This mutant protein is used to map the role of Glu^{112} on the maturation pathway of IMC-subtilisin.

Disruption of H Bonds between Glu^{112} in Subtilisin and the IMC Does Not Affect Catalysis—The E112A substitution was carried out in plasmids pET11a-WTpro-sub and pET11a-proS221Csub that contain wild-type IMC-subtilisin and IMC-S221C-subtilisin, respectively. Because the IMC-S221C-subtilisin can autoprocess but not degrade its IMC domain, amino acid substitutions within this construct enables one to analyze the effects of mutations on autoprocessing and the stability of the autoprocessed complex in the absence of IMC degradation (23). The wild-type and mutant precursors were expressed, purified, and refolded using a stepwise dialysis procedure established earlier (23, 31). Both IMC-subtilisin and IMC-E112A-subtilisin can undergo maturation to give active mature subtilisin (Fig. 2*A*). The secondary and tertiary structures of the 275-residue protease domain in both wild-type and E112A-subtilisin were monitored using CD spectroscopy. Fig. 2*B* indicates that the secondary structures of the two proteins are almost identical. E112A-subtilisin displays a very slight increase in the negative ellipticity at 208 nm. This suggests that the E112A substitution does not dramatically alter the secondary structure of the protease domain.

The tertiary structures of the two proteins were monitored using near UV-CD, and the spectra show similar patterns. However, E112A-subtilisin shows a reduction in the negative ellipticity at 278 nm (Fig. 2*C*). To ascertain change in the environments of the three tryptophan residues, two of which may be directly affected by the E112A substitution, the intrinsic fluorescence spectra of the two proteins were monitored (Fig. 2*D*). The proteins were excited at 295 nm, and the emission spectra of the proteins were recorded from 310 to 410 nm. The intrinsic fluorescence and near UV-CD spectra display small differences, and a reason for such changes can be attributed to perturbations in the α-helix within residues 104–116 caused by the E112A substitution. This residue is adjacent to Trp^{113} and in close proximity with Trp^{104}. The intrinsic fluorescence absorption at 350 nm increases by approximately 10% in case of E112A-subtilisin and suggests that local changes in tryptophan environment can occur as a result of the substitution. However, the overall secondary structures and the enzymatic properties of both wild-type and E112A-subtilisin are almost identical (Table I). Moreover, the two proteins also do not display exposed hydrophobic surface area that can bind with a fluorescent hydrophobic probe ANS (data not shown). It is important to note that although identical concentrations of precursors were utilized for folding, the yield of mature E112A-subtilisin is less than that of the wild-type subtilisin. Hence, the amount of the reaction mixture that had to be loaded in *lane 5* of Fig. 2*A* was 5-fold greater (by volume) than that for the wild-type subtilisin (Fig. 2*A*, *lane 3*). The mutant protease

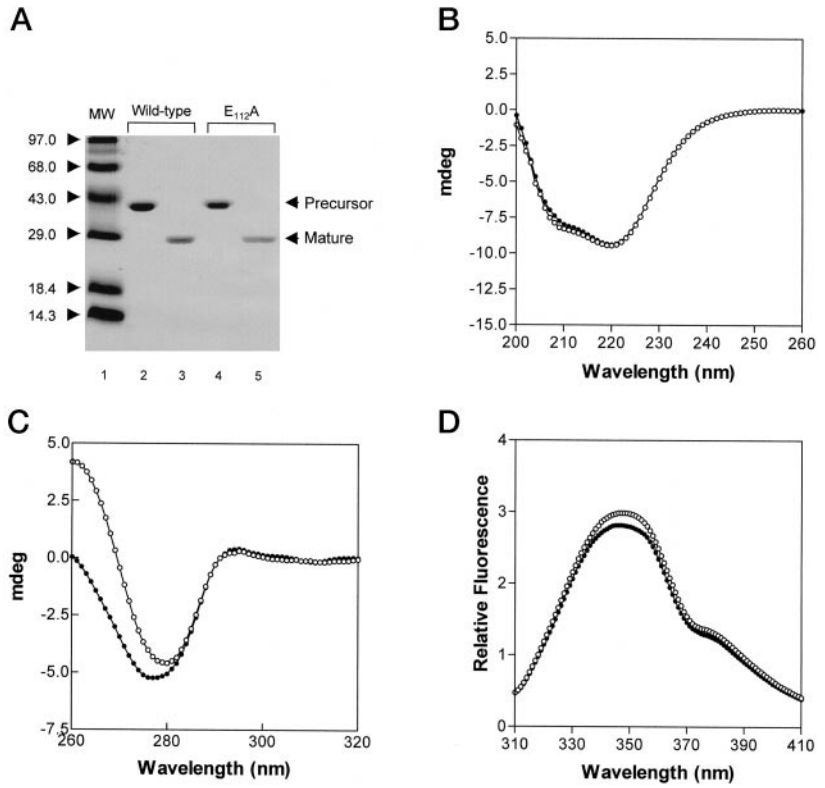

FIG. 2. **Characterization of wild-type and E112A-subtilisin.** *A*, renaturation of wild-type (*lane 2*) and E112A-subtilisin (*lane 4*) precursors by stepwise dialysis. After a 24-h incubation at 4 °C in the refolding buffer without urea, both precursors undergo maturation to give enzymatically active wild-type (*lane 3*) and E112A-subtilisin (*lane 5*). *Lane 5* represents a 5-fold greater volume of protein because the yield of mature E112A-subtilisin is significantly lower than that of the wild-type protein. *Lane 1* represents a molecular weight standard. *B*, far UV-CD spectra of wild-type subtilisin (*filled circles*) and E112A-subtilisin (*open circles*) show that the two proteins shown in *lanes 3* and *5* of *panel A* display almost identical secondary structures. *C*, near UV-CD spectra of the wild-type (*filled circles*) and E112A-subtilisin (*open circles*). The two proteins display slight differences in the near UV spectra. This is due to the effect of E112A substitution that may perturb the local environment of residues Trp^{106} and Trp^{113} that are located in an α-helical conformation. *D*, intrinsic fluorescence emission spectra of wild-type (*filled circles*) and E112A-subtilisin (*open circles*). The proteins were excited at 295 nm.

TABLE I
Enzymatic properterties of the wild-type and E112A-subtilisin

Property	E112A-subtilisin	Wild-type subtilisin
K_m	0.63 mM	0.59 mM
V_{max}	18 μM/min	21 μM/min
K_{cat}	17 s^{-1}	20 s^{-1}
K_i streptomyces for subtilisin inhibitor	15.5×10^{-9} M	8.5×10^{-9} M
Folding rate constant for precursor	0.0172 s^{-1}	0.0148 s^{-1}

melts approximately 2 °C lower than the wild-type protein as observed using CD spectroscopy (data not shown). This may be due to destabilization of α-helix 4 within subtilisin, and the lower yield of mature E112A-subtilisin may be attributed to its relative instability as compared with that of wild-type subtilisin. Hence, the Glu^{112} substitution within subtilisin allows the precursor to undergo maturation into an active protease domain with enzymatic properties almost identical to that of the wild-type subtilisin albeit with lower structural stability.

Disruption of H Bonds between Glu^{112} in Subtilisin and the IMC Affects Autoprocessing—To understand the role of the interface on the efficiency of autoprocessing, the E112A substitution was introduced in IMC-S221C-subtilisin. The proteins were expressed and purified as described earlier. IMC-E112A-S221C-subtilisin and IMC-S221C-subtilisin were renatured using stepwise dialysis against a buffer that contains reducing amounts of urea. Aliquots of the two proteins were removed at each stage of refolding and subjected to SDS-polyacrylamide gel electrophoresis (Fig. 3*A*). Under these refolding conditions approximately 70% of IMC-S221C-subtilisin undergoes autoprocessing. Fig. 3*A* indicates that upon reducing the urea concentration to 1 M, IMC-S221C-subtilisin begins to cleave its IMC domain. However, the IMC domain is not degraded and remains associated with the protease domain through noncovalent interactions. In case of IMC-E112A-S221C-subtilisin, the onset of cleavage is delayed, but efficiency of autoprocessing of both these precursors, in the absence of degradation of the IMC domain, reaches a maximum of 70% after 1 week of dialysis (Fig. 3, *A* and *C*). However, as discussed earlier, when mature E112A-subtilisin that harbors the wild-type active site was used, the yield of mature E112A-subtilisin was approximately 8-fold less than wild-type subtilisin under identical conditions (Fig. 2*A*). Because the active site variants IMC-S221C-subtilisin and IMC-E112A-S221C-subtilisin are only able to autoprocess but not degrade their IMC domains, whereas IMC-subtilisin and IMC-E112A-subtilisin can both autoprocess and degrade their IMC domains, the lower yield of subtilisin may occur as a consequence of intermolecular degradation of the precursor during refolding. Attempts to isolate the autoprocessed IMC-E112A-S221C-subtilisin complex from the unautoprocessed precursor for further biophysical characterization were unsuccessful. Concentration of the protein through ultra-filtration results in the precipitation of the E112A-S221C-subtilisin, whereas the unbound IMC domain remains in the supernatant (data not shown). This suggests that the interactions between the IMC domain and E112A-S221C-subtilisin appear to be much weaker than those observed in case of IMC-S221C-subtilisin complex. Therefore, the E112A substitution affects the rate of autoprocessing and stability of the autoprocessed complex.

To determine whether IMC-E112A-S221C- and IMC-S221C-subtilisin display any differences in their surface hydrophobicity, the proteins were examined for their ability to bind to ANS. It has been shown that ANS can specifically bind with exposed hydrophobic surfaces within proteins and has been extensively used to monitor the initiation of the folding process. Binding of ANS with the hydrophobic surfaces effects a shift in the fluorescence maxima from 560 to 490 nm, with a simultaneous increase in the fluorescence intensity at 490 nm that is proportional to the extent of exposed hydrophobic surface area within the protein. From Fig. 3*B* it is evident that IMC-E112A-S221C-subtilisin is more hydrophobic than IMC-S221C-subtilisin, and this increased hydrophobicity may facilitate the process of ag-

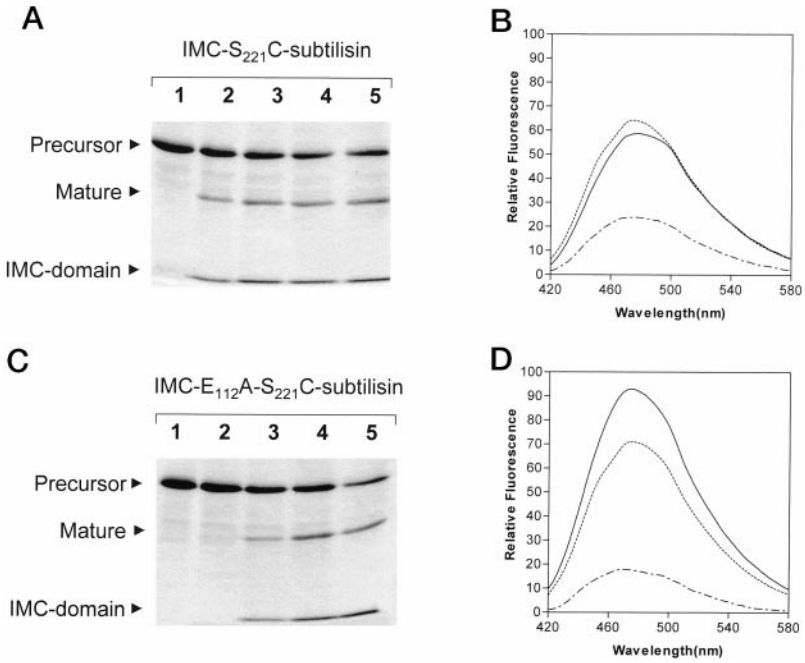

FIG. 3. **Characterization of the autoprocessed state in the maturation pathway of precursor proteins.** Autoprocessing of IMC-S221C-subtilisin (*A*) and IMC-E112A-S221C-subtilisin (*C*) using stepwise dialysis. Dialysis was carried out as described under "Experimental Procedures" against renaturing buffer (50 mM Tris-HCl, pH 7.0, 0.5M $(NH_4)_2SO_4$,1 mM $CaCl_2$, and 5 mM DTT) that contains 2.0 M urea (*lane 1*), 1.0 M urea (*lane 2*), 0 M urea for 24 h (*lane 3*), 0 M urea for 72 h (*lane 4*), and 0 M urea for 7 days (*lane 5*). Fluorescence because of binding of ANS with IMC-S221C-subtilisin (*B*) and IMC-E112A-S221C-subtilisin (*D*). The precursor proteins are represented by a *solid line* (0 M urea), the *dashed line* (1 M urea), and the *dashed* and *dotted line* (3 M urea). Data were collected as described under "Experimental Procedures."

gregation during the protein concentration. It is important to note that the increased ANS binding in the IMC-E112A-S221C-subtilisin does not occur as a result of different extents of autoprocessing. From Fig. 3 (*A* and *C*) it is evident that both E112A-S221C-subtilisin and S221C-subtilisin precursors autoprocess approximately 70% of their IMC domains after 1 week at 4 °C, which is consistent with published work (31).

Glu^{112} in Subtilisin Can Stabilize IMC Structure—Next, to obtain folded but inactive E112A-subtilisin to reconstitute a complex with the IMC domain, the following approach was taken. It has earlier been reported that PMSF-inhibited subtilisin can interact with the IMC domain to form a stable complex (37). Equimolar concentrations of the IMC domains were added to the PMSF-inhibited wild-type and E112A-subtilisins, and the mixtures were incubated for 1 h (at 4 °C) to allow complex formation. The secondary structures of the proteins were then analyzed using circular dichroism (Fig. 4*A*). The IMC-E112A-subtilisin complex displays an approximate 15% loss in ellipticity at 222 nm when compared with the wild-type complex. Because both mature wild-type and E112A-subtilisin display almost identical secondary structures, whereas the corresponding complexes with the IMC domain display discernable differences, it is reasonable to argue that the differences in the structures of the complex arise because of differences in their cognate IMC domains. Fig. 4*B* displays the differential spectra between the E112A-subtilisin and its complex compared with the IMC domain in the wild-type complex. Although the IMC domain complexed with wild-type subtilisin displays an α-β conformation, the IMC domain complexed with E112A-subtilisin displays a significantly different secondary structure. From Fig. 4*B* it appears that although not completely unfolded, the IMC domain in the E112A-subtilisin complex is significantly more unstructured. Therefore, it appears that the interaction between Glu^{112} and the peptide backbone of residues 40–43 within the IMC is critical for maintaining the IMC structure.

Disruption of H Bonds between Glu^{112} in Subtilisin and the IMC Does Not Alter Folding Initiation—It can, however, be argued that the Glu^{112} substitution may affect the initiation of the folding process. The folding kinetics of the precursor protein and its mutant can be monitored by rapidly diluting 200 μl of denatured IMC-subtilisin (1.25 mg/ml in 6 M guanidine hydrochloride, pH 4.8) and IMC-E112A-subtilisin into 2800 μl of renaturing buffer (50 mM Tris-HCl, pH 7.0, containing 0.5 M $(NH_4)_2SO_4$, 1 mM $CaCl_2$, 5 mM DTT) while simultaneously monitoring the changes in negative ellipticity at 222 nm using CD spectroscopy as described under "Experimental Procedures." CD spectroscopy provides an excellent tool for following the changes in secondary structure during the process of folding/unfolding if the changing states are not themselves completely defined. It is important to note that enzymatic activity of wild-type IMC-subtilisin can be observed approximately 3 h after folding. Therefore, the overall maturation kinetics of IMC-subtilisin appear to be slow and can be monitored using manual mixing methods. The dead time of this experiment was approximately 1 s, and the final CD signal of the wild-type precursor protein after 1 h of refolding was approximately 95% of the total signal that obtained upon complete refolding (Fig. 5*A*). The folding traces for both IMC-subtilisin and IMC-E112A-subtilisin can be fitted to a single exponential rate

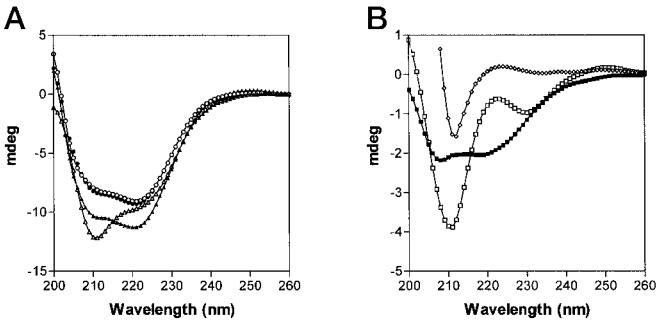

FIG. 4. **Structural characterization of IMC domains complexed with wild-type and E112A-subtilisin.** *A*, the far UV-CD spectra of the mature proteins that are first inhibited using PMSF. Wild-type mature subtilisin (*filled circles*) displays an almost identical secondary structure to mature E112A-subtilisin (*open circles*). However, the IMC-E112A-subtilisin complex (*open triangles*) displays a significantly different structure from that of the wild-type complex (*filled triangles*). *B*, difference spectra between the mature proteins and their complexes with the IMC domain. The secondary structure of the IMC domain in the presence of the wild-type protein (*filled squares*) is more organized than that in a complex with E112A-subtilisin (*open squares*). The IMC domain that is denatured by 6 M guanidine hydrochloride is depicted by *open diamonds*.

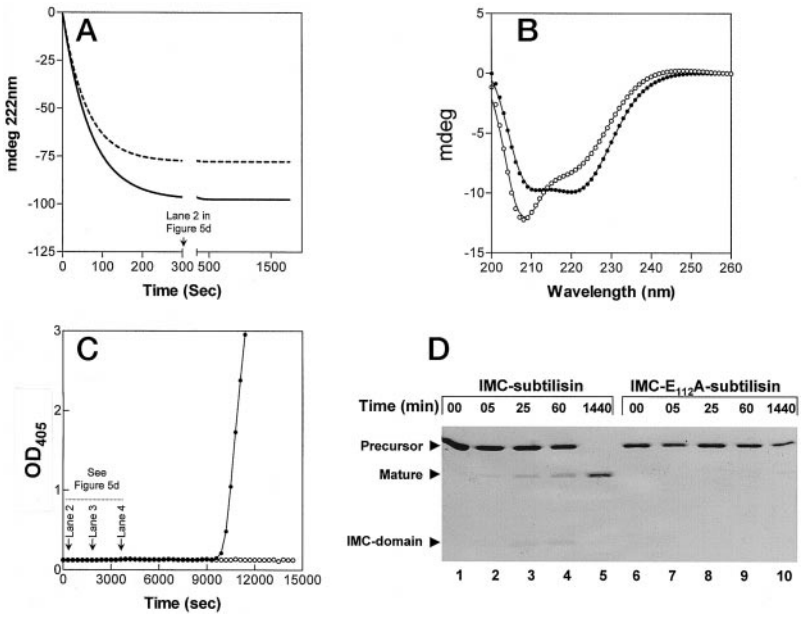

FIG. 5. **Characterization of folding of IMC-subtilisin and IMC-E112A-subtilisin.** *A*, folding kinetics of IMC-subtilisin (*solid line*) and IMC-E112A-subtilisin (*dashed line*). Folding was initiated by rapid dilution into 50 mM Tris-HCl, pH 7.0, containing 0.5 M $(NH_4)_2SO_4$, 1 mM $CaCl_2$, and 5 mM DTT as described under "Experimental Procedures." Changes in the negative ellipticity at 222 nm were monitored using CD spectroscopy. *B*, the secondary structure of the IMC-subtilisin (*filled circles*) and IMC-E112A-subtilisin (*open circles*). *C*, release of inhibition through degradation of the IMC domain by IMC-subtilisin (*filled circles*) and IMC-E112A-subtilisin (*open circles*). 6 μl of denatured IMC-subtilisin and IMC-E112A-subtilisin (1.25 mg/ml each) were rapidly diluted into 50 mM Tris-HCl, pH 7.0, containing 0.5 M $(NH_4)_2SO_4$, 1 mM $CaCl_2$, 5 mM DTT, and 1 mM *N*-succinyl-Ala-Ala-Pro-Phe-*p*-nitroanilide. Subtilisin activity was monitored at 405 nm as a function of time. *D*, autoprocessing of IMC-subtilisin and IMC-E112A-subtilisin monitored using 15% SDS-polyacrylamide gel electrophoresis. Aliquots of 50 μl of protein were removed at the designated time intervals and added into 6 μl of 100% trichloroacetic acid to terminate the reaction.

equation using the Graph-Pad software. The folding rate constants obtained from fitting the above data are 0.0148 ± 0.005 and 0.0172 ± 0.0004 for IMC-subtilisin and IMC-E112A-subtilisin, respectively. Fig. 5*B* displays the secondary structure of the proteins after 1 h of rapid dilution. Both IMC-subtilisin and IMC-E112A-subtilisin display significant secondary structures. Moreover, the secondary structure of IMC-subtilisin is native-like and similar to that of the autoprocessed complex that has been crystallized. However, IMC-E112A-subtilisin displays a 15% decrease in ellipticity at 222 nm and a concomitant increase in ellipticity at 208 nm and is consistent with the complex obtained by addition of the IMC domain *in trans* (Fig. 4*A*).

Fig. 5*D* monitors the autoprocessing activity of the protease domain under conditions identical to those employed in the rapid dilution experiments. As evident from Fig. 5*D*, wild-type precursor autoprocesses an indiscernible amount of its precursor within the time scale of the rapid dilution experiment (*lane 2*). After approximately 1 h of rapid dilution, the precursor autoprocesses approximately 4–5% of its IMC domain (Fig. 5*D*). Under identical conditions, proteolytic cleavage of the synthetic substrate does not occur, although efficient autoprocessing can transpire (Fig. 5, *C* and *D*). The substrate binding loop and the active site residues, in both unautoprocessed as well as autoprocessed complex, are not accessible to protease inhibitors like streptomyces subtilisin inhibitor or PMSF (3). Such inhibitors are therefore known to be unable to block autoprocessing and degradation of the IMC domain (3). Therefore, the active site of subtilisin in either an unautoprocessed or autoprocessed complex cannot degrade precursor molecules intermolecularly, unless it first degrades its inhibitory IMC domain. Because intermolecular proteolytic activity is not evident during the time scale of the refolding experiments, loss in CD spectroscopic signal because of degradation does not occur and will not hamper the monitoring of refolding kinetics of IMC-subtilisin during the time scale of the experiment. Proteolytic cleavage of a synthetic substrate *N*-succinyl Ala-Ala-Pro-Phe-*p*-nitroanilide was monitored to determine the onset of mature subtilisin devoid of its inhibitory IMC domain. Fig. 5*C* depicts the occurrence of the mature protease domain as a function of time for both IMC-subtilisin and IMC-E112A-subtilisin. The wild-type precursor can degrade its IMC domain to release enzymatic activity in approximately 3 h after rapid dilution. Under these conditions the precursor has undergone approximately 20% autoprocessing. However, IMC-E112A-subtilisin does not undergo auto-proteolytic cleavage during the 3-h period (Fig. 5*C*). After an overnight incubation at 4 °C, the wild-type precursor undergoes complete maturation, whereas the IMC-E112A-subtilisin shows minor traces of autoprocessing. Based on Fig. 5, we suggest the disruption of the hydrogen bonds between Glu^{112} within subtilisin and the peptide backbone of the IMC domain does not dramatically alter the folding initiation of the precursor proteins. However, Glu^{112} significantly alters autoprocessing of the precursor protein and suggests that the hydrogen bonding between Glu^{112} and the IMC domain is not important for the overall folding process but occurs late during the folding pathway to affect autoprocessing of the IMC. This is consistent with data that show the structure of the IMC-subtilisin complex before and after autoprocessing is different (23, 24, 28). These results also suggest that degradation of the IMC domain appears to be the rate-limiting step in the maturation pathway.

Glu^{112} in Subtilisin Is Critical for the Inhibitory Function of the IMC Domain—To investigate the role of Glu^{112} in the binding of the IMC with the protease domain, the ability of the IMC to inhibit protease activity was determined. The enzymatic activity of both the wild-type and E112A-subtilisin are similar (Table I). Equal units of wild-type and E112A-subtilisin were inhibited using 6.0–8.0 μM of the IMC domain. Fig. 6*A* depicts the release of inhibition as a function of time. E112A-subtilisin degrades the different concentrations of the IMC domain very easily, and enzymatic activity can be observed

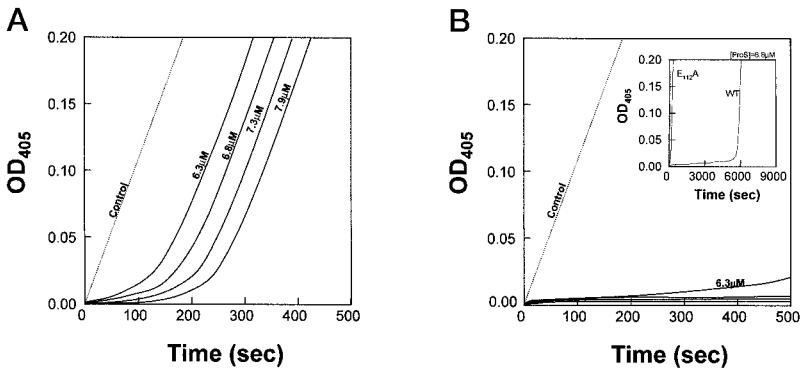

FIG. 6. **Release in inhibition caused by degradation of wild-type IMC domain by wild-type and mutant subtilisin.** *A* and *B*, degradation of *N*-succinyl Ala-Ala-Pro-Phe-*p*-nitroanilide observed by change in absorption at 405 nm because of release of *p*-nitroanilide by E112A-subtilisin (*A*) and wild-type subtilisin (*B*). Wild-type subtilisin is completely inhibited within the depicted time scale. Therefore, the degradation of the 6.8 μM IMC domain by E112A-subtilisin and wild-type subtilisin are shown as an *inset* to *panel B*. The *dashed line* represents equal units of uninhibited E112A and wild-type subtilisin. E112A-subtilisin degrades 6.8 μM of the IMC domain within 170 s, whereas the wild-type subtilisin degrades 6.8 μM of the IMC within 6000 s. Therefore, the E112A substitution reduces its affinity for the IMC by approximately 35-fold.

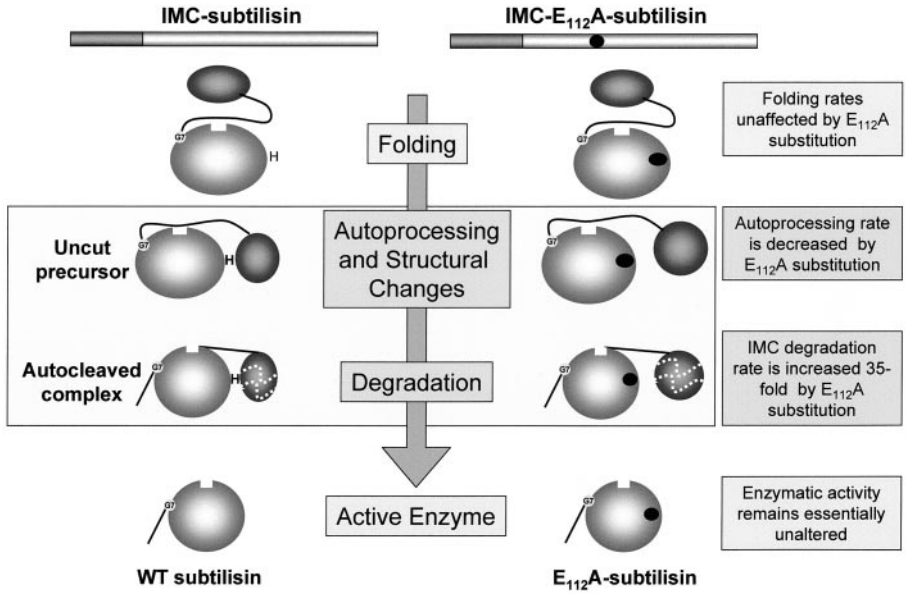

FIG. 7. **A schematic representation of how E112A substitution affects the maturation pathway of the precursor.** The *black circles* depict the mutation, whereas *H* symbolizes the hydrogen bonds between Glu^{112} and the IMC domain.

within 2 min for 6.3 μM concentration. Within 10 min of the addition of E112A-subtilisin, complete degradation of the IMC domain occurs, and the velocity of substrate degradation equals that of the uninhibited protease. However, in the case of wild-type subtilisin, the release in inhibition is dramatically slower. As evident from the *inset* in Fig. 6*B*, wild-type subtilisin degrades 6.8 μM of the IMC domain in approximately 6000 s, whereas the same units of mature E112A-subtilisin degrades the IMC domain in approximately 170 s. Although the exact inhibition constant of the IMC domain for E112A-subtilisin has not been estimated, these results show that E112A-subtilisin degrades the IMC domain approximately 35-fold faster than the wild-type protein. Hence, the interactions between the side chain of Glu^{112} and the backbone of the residues 42–44 within the IMC domain are important for binding of the IMC with the protease domain. This residue, however, does not significantly affect the binding of the streptomyces subtilisin inhibitor with the protease domain (Table I).

Conclusions—Based on the data presented in this manuscript both, IMC-subtilisin and IMC-E112A-subtilisin display similar folding rate constants (Table I). It has been shown by Bryan and co-workers (38) that when the IMC domain is added *in trans,* the rate-limiting step of folding is the formation of the initial IMC-subtilisin collision complex. Our results seem to be consistent with this hypothesis. However, because of the covalent linkage between the IMC domain and the enzymatic domain, the rate constant of collision complex formation may be higher in our system. Moreover, the interactions that stabilize the IMC-subtilisin complex may not necessarily be those required for the initiation of folding. Therefore, the Glu^{112} H bonding with the backbone of the IMC domain is not critical for initiating protein folding and does not seem to be involved in the collision complex. However, the hydrogen bonding between Glu^{112} and the IMC backbone is important for efficient autoprocessing (Fig. 7). In the absence of this interaction, the uncleaved IMC domain fluctuates dynamically and possibly destabilizes the interactions between the C terminus of the IMC domain and the substrate-binding loop in subtilisin, which is critical for autoprocessing. As a result the IMC-E112A-subtilisin precursor cleaves its IMC domain much slower than IMC-subtilisin. Upon cleavage from the N terminus of subtilisin, the IMC domain remains noncovalently associated with the protease domain. This tight association seems to be responsible for the inhibitory functions of the IMC domain. The E112A substitution dramatically reduces the binding of the IMC domain with subtilisin by approximately 35-fold. E112A-subtilisin displays similar activities (Table I) toward synthetic peptide substrates and shows an affinity toward streptomyces subtilisin

inhibitor that is similar to that observed with wild-type subtilisin.

Therefore as summarized in Fig. 7, we suggest that (i) the interaction between Glu^{112} and the IMC domain is not critical for initiating the folding process but is critical for maintaining the IMC domain in an autoprocessing competent state; (ii) the removal of the IMC domain from the protease domain is the rate-limiting step in the maturation of IMC-subtilisin; and (iii) the wild-type IMC domain is a very weak inhibitor of E112A-subtilisin but maintains its ability to facilitate correct folding. Hence, the ability of the IMC domain to fold subtilisin into an active conformation does not necessarily correlate with its ability to inhibit the enzymatic activities of subtilisin as proposed earlier.

Acknowledgment—We are grateful to Drs. Sangita Phadtare and Cynthia Marie-Claire for suggestions and for reading this manuscript.

REFERENCES

1. Wong, S. L., and Doi, R. H. (1986) *J. Biol. Chem.* **261,** 10176–10181
2. Ikemura, H., Takagi, H., and Inouye, M. (1987) *J. Biol. Chem.* **262,** 7859–7864
3. Ikemura, H., and Inouye, M. (1988) *J. Biol. Chem.* **263,** 12959–12963
4. Zhu, X., Ohta, Y., Jordan, F., and Inouye, M. (1989) *Nature* **339,** 483–484
5. Shinde, U. P., and Inouye, M. (1993) *Trends Biochem. Sci.* **18,** 442–446
6. Barr, P. (1991) *Cell* **66,** 1–3
7. Silen, J. L., and Agard, D. A. (1989) *Nature* **341,** 362–264
8. Baker, D., Sohl, J. L., and Agard, D. A. (1992) *Nature* **356,** 263–265
9. Lee Y. C., Miyata, Y., Terada, I., Ohta, T., and Matsuzawa, H. (1991) *Agric. Biol. Chem.* **55,** 3027–3032
10. Kwon S. T., Terada, I., Matsuzawa, H., and Ohta, T. (1988) *Eur. J. Biochem.* **73,** 1–7
11. Sørensen, P., Winther, J. R., and Kaarsholm, N. C. (1993) *Biochemistry* **32,** 12160–12166
12. Winther, J. R., and Sørensen, P. (1991) *Proc. Natl. Acad. Sci. U. S. A.* **88,** 9330–9334
13. Smith, S. M., and Gottesman, M. M. (1989) *J. Biol. Chem.* **264,** 20487–20495
14. Marie-Claire, C., Ruffet, E., Beaumont, A., and Roques B. P. (1999) *J. Mol. Biol.* **285,** 1911–1915
15. Suter, U., Angst C., Tien, C. L., Drinkwater, C. C., Lindsay, R. M., and Shooter, E. M. (1992) *J. Neurosci.* **12,** 306–318
16. Thorne, B. A., and Plowman G. D. (1994) *Mol. Cell. Biol.* **14,** 1635–1646
17. Gray, A. M., and Mason, A. J. (1990) *Science* **247,** 1328–1330
18. Eder, J., and Fersht, A. R. (1995) *Mol. Microbiol.* **16,** 609–614
19. Shinde, U. P., Liu, J. J., and Inouye, M. (1997) *Molecular Chaperones in the Life Cycle of Proteins*, 1st Ed., pp. 467–490, 2000, 11(1), 3544, Marcel Dekker, Inc., New York
20. Shinde, U. P., and Inouye, M. (2000) *Semin. Cell Dev. Biol.* **11,** 35–44
21. Shinde, U. P, and Inouye, M. (1994) *J. Biochem.* (*Tokyo*) **115,** 629–636
22. Shinde, U. P., Li Y., Chatterjee S., and Inouye, M. (1993) *Proc. Natl. Acad. Sci. U. S. A.* **90,** 6924–6928
23. Shinde, U. P., and Inouye, M., (1995) *J. Mol. Biol.* **252,** 25–30
24. Shinde, U. P., and Inouye, M. (1995) *J. Mol. Biol.* **247,** 390–395
25. Eder, J., Rheinnecker, M., and Fersht, A. (1993) *Biochemistry* **32,** 18–26
26. Eder, J., Rheinnecker, M., and Fersht, A. (1993) *J. Mol. Biol.* **233,** 293–304
27. Shinde, U. P., Liu, J. J., Inouye, M. (1997) *Nature* **389, 5**20–522
28. Shinde, U. P., Fu, X., Inouye, M. (1999) *J. Biol. Chem.* **274,** 15615–15621
29. Ellis, R. B. (1998) *Trends Biochem. Sci.* **23,** 43–45
30. Prusiner, S. B. (1998) *Proc. Natl. Acad. Sci. U. S. A.* **95,** 13363–13383
31. Li, Y., and Inouye, M. (1994) *J. Biol. Chem.* **269,** 4169–4174
32. Gallagher, T., Gilliland, G., Wang, L., and Bryan, P. (1995) *Structure* **3,** 907–914
33. Jain, S. C., Shinde, U. P., Li, Y, Inouye, M., and Berman, H. M. (1998) *J. Mol. Biol.* **284,** 137–144
34. Li, Y., Hu, Z., Jordan, F., and Inouye, M. (1995) *J. Biol. Chem.* **270,** 25127–25132
35. Bryan, P. (1995) *Intramolecular Chaperones and Protein Folding* (Shinde, U. P., and Inouye, M., eds) R. G. Landes Company, Austin, TX
36. Bryan, P., Wang, L., Hoskins, J., Ruvinov, S, Strausberg, S., Alexander, P, Almog, O., Gilliland, G., and Gallagher, T. (1995) *Biochemistry* **34,** 10310–10318
37. Hu, Z., Haghjoo, K., and Jordan, F. (1996) *J. Biol. Chem.* **271,** 3375–3384
38. Strausberg, S., Alexander, P., Wang, L., Schwarz, F., and Bryan, P. (1993) *Biochemistry* **32,** 8112–8119